14C.6

DIURNAL VARIATION OF UPPER TROPOSPHERIC HUMIDITY OVER THE TROPICS AND ITS RELATIONS TO CONVECTIVE ACTIVITIES

Eui-Seok Chung[1], Byung-Ju Sohn[1,*], and Johannes Schmetz[2]
[1]Seoul National University, Seoul, Korea
[2]EUMETSAT, Darmstadt, Germany

1. INTRODUCTION

Diurnal variation, which is related to the large and well-defined cycle in solar heating during the day, is one of the most fundamental components accounting for the variability of the climate system. Numerous observation studies have documented diurnal variation of deep convection, precipitation, cloudiness, and outgoing longwave radiation over the tropics (e.g., Gray and Jacobson, 1977; Duvel and Kandel, 1985; Hendon and Woodberry, 1993; Chen and Houze, 1997; Yang and Slingo, 2001; Nesbitt and Zipser, 2003 among many others). Previous studies agree that the amplitude of the diurnal variation is larger over land than over open oceans and most land regions attain diurnal maxima in the afternoon to evening. However, significant differences in the timing of diurnal maximum have been reported over the ocean, resulting in various hypotheses for explaining the observed phenomena (Gray and Jacobson, 1977; Randall et al., 1991; Chen and Houze, 1997; Dai, 2001).

Although the variability of water vapor at longer time scales has been investigated (e.g., Bates et al., 2001), few studies examined the diurnal variation of water vapor despite its link with deep convection and cloudiness. This lack of study is worse for water vapor in the upper troposphere, due to the poor spatial and temporal sampling from conventional radiosonde measurements. Dai et al. (2002) analyzed three-hourly specific humidity data from one radiosonde site (the Atmospheric Radiation Program (ARM) Cloud and Radiation Testbed (CART) site near Lamont, Oklahoma), and found that water vapor above around 2 km typically peaks around 0300 local time in all seasons. Near the surface, water vapor minima occurred in the morning in all seasons except summer.

The poor sampling problem has been somewhat reduced by using more frequent measurements of water vapor channel radiances from geostationary satellites. For the first time, Udelhofen and Hartmann (1995) tried to study the diurnal variation of upper tropospheric humidity (UTH) from GOES-7 6.7 μm radiances and showed the close association with that of high cloudiness. Using GOES-7 6.7 μm radiances, Soden (2000) reported a clear-contrast in phase relationship between land and ocean. While the variation in high cloudiness and UTH tended to occur in phase with changes in deep convection over land, there exists a nearly 12 hour out-of-phase relationship with changes in deep convection over ocean. Tian et al. (2004) documented the diurnal phase relationships from a new data set constructed from global, 3-hourly water vapor and window radiances from multiple geostationary satellites. They found that the diurnal cycle in UTH is stronger over land than over ocean and that UTH tends to peak around the midnight over ocean in contrast to 0300 local time over land.

Although Tian et al. (2004) documented the diurnal cycle of UTH over the whole tropics, more studies for different time periods with different datasets are required to draw a general conclusion on diurnal variation of UTH and its relations to deep convection and cloudiness. This study intends to document the diurnal variation of UTH (and middle tropospheric humidity) and its relations to deep convection and high cloudiness over the tropical Indian Ocean and tropical Africa using European Geostationary Meteorological Satellites (i.e., Meteosat 5 and 8) measurements.

2. DATA AND METHOD

2.1 *Data*

In the later part of the Meteosat-5 observation, it was located at 63ºE on the equator, and observed the earth every half-an hour in three spectral bands: visible channel (0.3-1.05 μm), infrared window channel (10.5-12.5 μm), and water vapor channel (5.7-7.1 μm). In this study, Meteosat-5 measured count values (0.25º gridded data obtained from the

* *Corresponding author address:*
Prof. B.J. Sohn
School of Earth and Environmental Sciences
Seoul National University, Seoul, 151-747, Korea
E-mail: sohn@snu.ac.kr
Phone: +82-2-880-7783, Fax: +82-2-872-8156

Laboratoire de Meteorlogie Dynamique (LMD) of France), were converted into equivalent blackbody temperatures, by applying the calibration coefficients provided by EUMETSAT. Three-hourly equivalent blackbody temperatures from the water vapor and infrared window channel measurements were used for July 1998 over the tropical Indian Ocean including the Indian subcontinent (30ºN-30ºS, 30ºE-110ºE). The warm bias of water vapor channel is adjusted by subtracting 3 K from observed brightness temperature (Sohn et al., 2000).

Hourly Meteosat-8 infrared measurements are also employed. Meteosat-8, currently orbiting above a longitude of 0º, observes the full disk of the earth with an imaging repeat cycle of 15 minutes. Spinning Enhanced Visible and Infrared Imager (SEVIRI) onboard Meteosat-8 observes the earth-atmosphere system with 12 channels: eight channels in the thermal infrared at 3.9, 6.2, 7.3, 8.7, 9.7, 10.8, 12.0 and 13.4 μm, three channels in the shortwave region at 0.6, 0.8, and 1.6 μm, and a broad-band high resolution visible channel. Spectral channel characteristics of SEVIRI are described in more detail in Schmetz et al. (2002). Besides radiances from 6.2 μm and 10.8 μm channels used for cloud classification and UTH estimation as in Meteosat-5, 7.3 μm channel measurements are also used for the middle tropospheric humidity (MTH). The Level 1.5-image data for July 2004 are analyzed over central African area, including the adjacent tropical Atlantic Ocean (30ºN-30ºS, 50ºW-50ºE).

2.2 *Precipitation Index, High Cloud, and UTH*

The window channel equivalent blackbody temperature (TB_{11}) is used to roughly define deep convection and high cloud fraction. Hendon and Woodberry (1993) developed the index of deep convection by relating brightness temperature to an equivalent precipitation rate. Following Hendon and Woodberry (1993) and Tian et al. (2004), precipitation index (PI) is employed to infer the tropical precipitation associated with deep convection. The precipitation index (unit: mm day^{-1}) is defined as follows, based on an empirical relationship that clouds with colder cloud top temperature are more closely associated with heavier precipitation:

$$PI = a(230 - TB_{11}), \text{ if } TB_{11} < 230 \text{ K}. \quad (1)$$

The proportionality constant (a), derived for the time-mean of the zonal average throughout the tropics, was assumed to hold locally as well as instantaneously (Hendon and Woodberry, 1993). Temperature threshold of 260 K is used to infer high cloudiness (Chen and Houze, 1997; Tian et al., 2004). High cloud cover is defined as the percentage of pixels in a 2.5˚×2.5˚ grid box, and consists of deep convective clouds (TB_{11} < 230 K) and cirrus anvil clouds (230 K < TB_{11} < 260 K).

The UTH, defined as the mean relative humidity over a layer between about 500 hPa and 200 hPa in the clear sky, is related to the brightness temperatures of water vapor channel. It was shown that the water vapor channel brightness temperature (T_{WV}) is linearly related to the natural logarithm of UTH divided by the cosine of the viewing angle (Soden and Bretherton, 1993). The relationship is as follows:

$$\ln (UTH/\cos \theta) = a + bTB_{WV}. \quad (2)$$

The dependence of water vapor channel brightness temperatures on atmospheric temperature is considered to improve the quality of the statistical coefficients computations (Schmetz et al., 1995). To obtain the linear coefficients (a and b) incorporating the effect of local temperature lapse rate, temperature profiles from NCEP/NCAR Reanalysis (Kalnay et al., 1996) are used as an input to a radiative transfer calculation. UTH estimations are limited to the low cloud or cloud-free area. For July 2004, a linear relationship as shown in Eq. (2) is also applied to Meteosat-8 7.3 μm channel brightness temperatures to estimate MTH.

2.3 *Data Analysis*

Harmonic analysis is used to study the diurnal variations of deep convection, high cloud, and free tropopsheric humidity (UTH and MTH). A composite day was first constructed by averaging these fields at fixed time intervals (e.g., 3 hours or 1 hour) from each day at each grid point. Then, the amplitude and phase of the first diurnal (24 hour) harmonic are obtained by decomposing the resulting composite day through Fourier analysis. The diurnal phase corresponds to the local time showing a maximum of the variable in interest. The diurnal amplitude and phase are represented by harmonic dial which depicts two parameters of a single harmonic using a line segment. The length and angular orientation (or pointing direction) of the line indicate amplitude and phase angle, respectively.

3. RESULTS

3.1 *Tropical Indian Ocean*

Geographical distributions of monthly mean window channel brightness temperature (TB_{11}) and UTH for July 1998 are represented in Fig. 1.

Monthly mean 200 hPa wind fields from NCEP/NCAR Reanalysis are superposed on the UTH fields. The distribution of TB_{11} clearly shows convectively active regions (TB_{11} < 270 K) such as the Indian subcontinent, the Bay of Bengal, and the intertropical convergence zone (ITCZ). The close resemblance between cold TB_{11} (< 270 K) and high UTH (> 40%) implies that detrainment of hydrometeors from high clouds could contribute to the moistening of the upper tropopshere (Sohn and Schmetz, 2004). UTH rapidly decreases with distance from the convective regions (Udelhofen and Hartmann, 1995). The comparison of wind fields and UTH distributions indicates that the subsiding branches of Hadley-type circulation are influenced by the adjacent convective region through the large-scale advection.

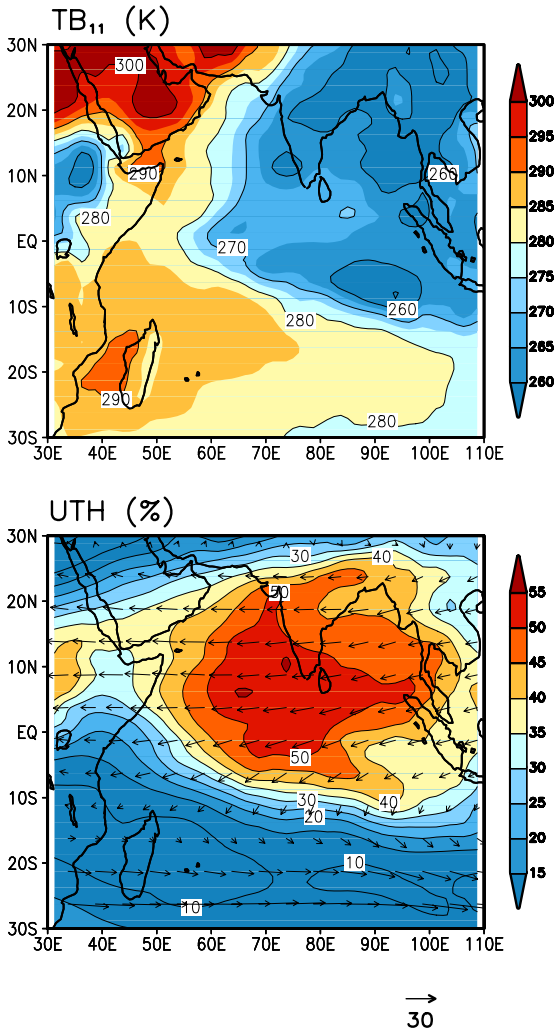

Figure 1: Geographical distributions of monthly mean TB_{11} (top) and UTH (bottom) for July 1998. The 200 hPa wind fields (unit: m s^{-1}) from NCEP/NCAR Reanalysis are superposed on the distribution of UTH.

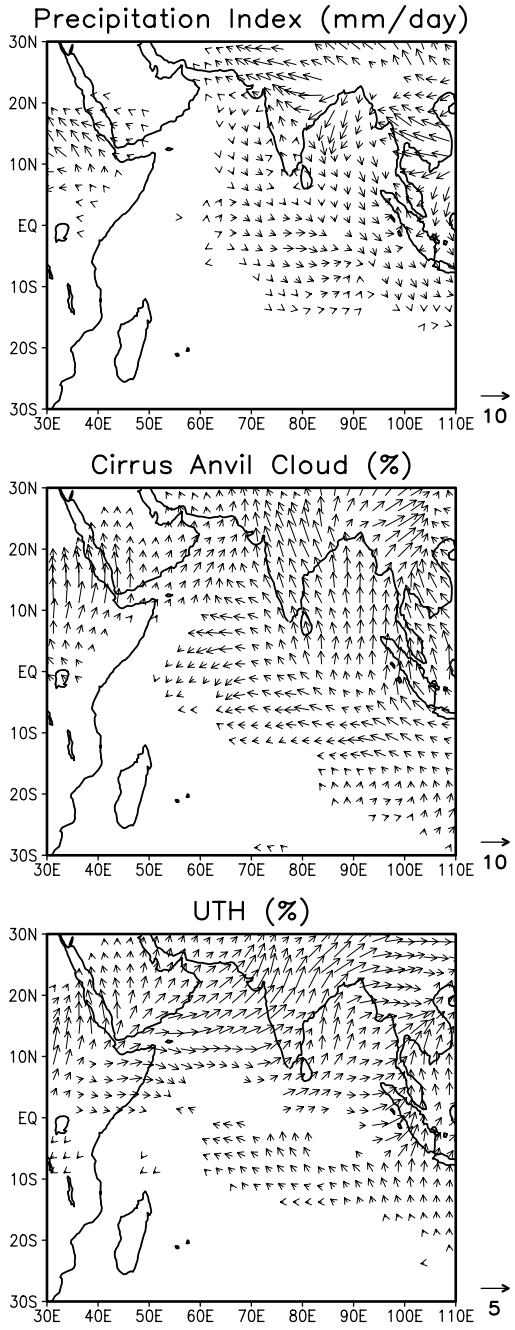

Figure 2: Diurnal amplitudes and phases of precipitation (top), cirrus anvil cloud (middle), and UTH (bottom) for July 1998. The units are mm day^{-1} for precipitation and % for cirrus anvil clouds and UTH. The length of the arrow depicts the diurnal amplitudes (10 mm day^{-1} for precipitation, 10% for cirrus anvil cloud, and 5% for UTH).

Fig. 2 represents the diurnal amplitudes and phases of precipitation index (top), cirrus anvil cloud (middle), and UTH (bottom) estimated from Meteosat-5 infrared channel measurements. The length of the arrow indicates the diurnal amplitude of each variable. The phase corresponds to the local time of maximum and

can be determined from the orientation of the arrow with respect to a 24-hour clock. For example, arrows pointing upward indicate a peak at 0000 local time (LT), toward the right indicate a peak at 0600 LT (dawn), downward indicate a peak at 1200 LT (noon), and toward the left indicate 1800 LT (sunset).

Large diurnal variations in deep convection are observed over Ethiopian highlands and Asian Monsoon regions as noted in other studies (i.e., Duvel and Kandel, 1985; Duvel, 1989; Gambheer and Bhat, 2001; Nesbitt and Zipser, 2003). The peak of precipitation occurs in the late afternoon and early evening (1800-2100 LT) over land. In contrast, open ocean shows relatively weaker variation and the maximum rainfall tends to occur during early morning hours. Morning preference of oceanic rainfall is consistent with the previous studies using passive microwave precipitation data (Imaoka and Spencer, 2000; Nesbitt and Zipser, 2003). Peaks around noon are frequent over coastal regions including the Bay of Bengal, implying land influences (Gambheer and Bhat, 2001; Zuidema, 2003).

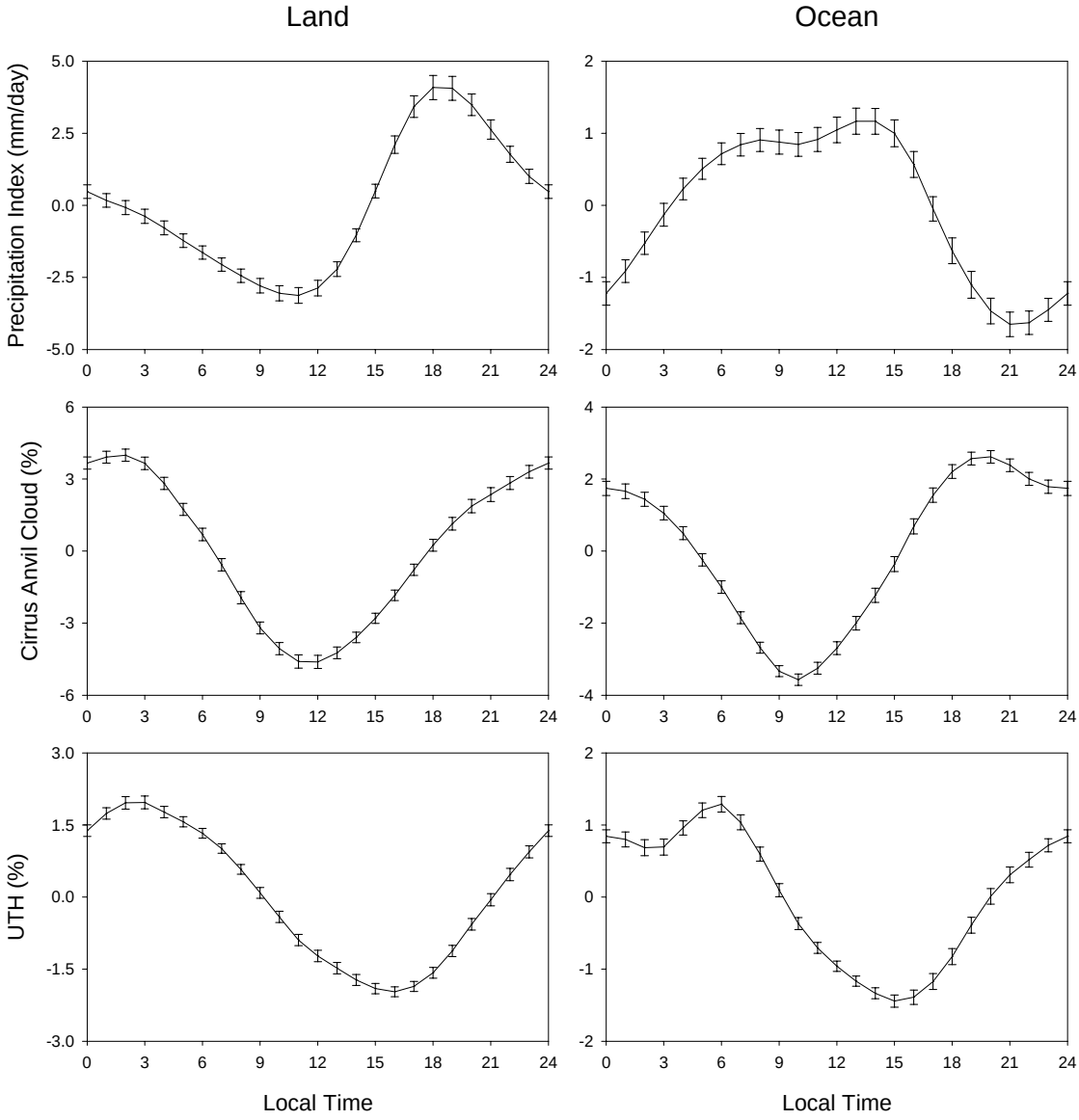

Figure 3: Average diurnal anomalies in precipitation (mm day^{-1}), cirrus anvil cloud (%) and UTH (%) for spatial averages over land regions (left) and ocean regions (right) in July 1998. Vertical bars represent the standard errors for each hourly mean.

Cirrus anvil clouds also show a clear land-sea contrast. Large diurnal variations are found over Ethiopian highlands and Asian monsoon regions with peaks around midnight (Duvel, 1989; Gambheer and Bhat, 2001, Tian et al., 2004). Over land, diurnal variations of high

clouds (not shown) are similar to those of cirrus anvil clouds except for a few hours earlier peaks. On the other hand, oceanic cloudiness (both high clouds and cirrus anvil clouds) show weaker diurnal amplitudes and peaks around 1800 LT (Kondragunta and Gruber, 1996; Tian et al., 2004). Land influences can be identified near coastal regions.

Convectively active regions have a discernible diurnal variation in UTH with larger amplitude over land (Udelhofen and Hartmann, 1995; Soden, 2000; Tian et al., 2004). A land-sea contrast in the timing of maximum is revealed. While UTH tends to peak in the nighttime (0100-0400 LT) over land, UTH maxima occur around 2100 LT over open ocean. Arabian Sea and the Bay of Bengal show nighttime peaks. General behavior of the UTH diurnal cycle is consistent with the results of Soden (2000) and Tian et al. (2004). By contrast, Udelhofen and Hartmann (1995) reported peaks around 0600 LT.

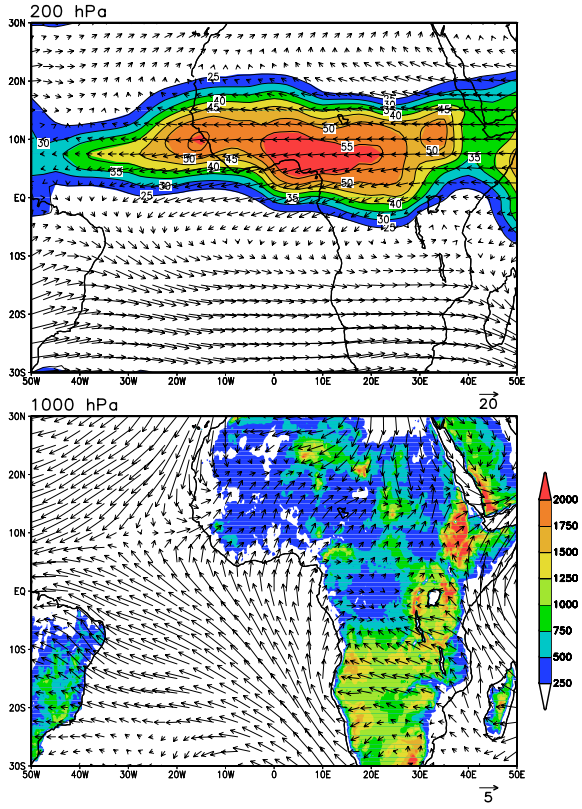

Figure 4: Monthly mean (July 2004) wind fields at two vertical levels (upper: 200 hPa, lower: 1000 hPa) from NCEP/NCAR reanalysis. Monthly mean UTH (unit: %) and surface elevation (unit: m) are superposed on the 200 hPa winds and the 1000 hPa winds, respectively.

The average diurnal anomalies of precipitation, cirrus anvil cloud (and high cloud), and UTH are compared in Fig. 3. Vertical bars represent the standard error for each hourly mean. Grid boxes with the diurnal standard deviation of UTH less than 1 % are excluded to reduce fluctuation irrelevant to diurnal variation. Fig. 3 shows a clear land-sea contrast in the phase of diurnal variations, besides the differences in the amplitudes of diurnal anomalies. Over land, both precipitation and high clouds (not shown) attain maxima in the late afternoon (~1800 LT) and minima before noon. Despite similar time of minimum, cirrus anvil cloud appears to lag precipitation and high clouds with a peak at near 0200 LT. This time lag suggests that higher (and colder) clouds might evolve to lower (and warmer) clouds during the nighttime. UTH tends to peak around 0300 LT and to have minimum a few hours earlier than the timing of precipitation maximum. This time of peak is very similar to the UTH peak from radiosonde humidity measurements (Dai et al., 2002).

Over ocean, diurnal variation in precipitation shows dual peaks (early morning and early afternoon), resulted from one peak over open oceans and the other peak over coastal regions. High clouds and cirrus anvil clouds, however, have one nearly identical peak in late afternoon (~1800 LT), indicating weaker convective intensity compared to land cases. In addition to maximum in the early morning, average diurnal anomaly of UTH shows a broad secondary peak during the midnight. The timing of minimum is nearly identical to that of land UTH.

3.2 *Tropical Africa*

Metesat-8 observations in July 2004 are analyzed for documenting diurnal variation of deep convection, high cloud, and UTH over tropical Africa and adjacent Atlantic Ocean. Diurnal variation of MTH is also investigated with additional 7.3 μm channel of Meteosat-8. Monthly mean wind fields at two vertical levels (200 and 1000 hPa) from NCEP/NCAR reanalysis are plotted in Fig. 4. Monthly mean UTH (unit: %) and surface elevation (unit: m) are superposed on the 200 hPa wind and 1000 hPa wind, respectively. Surface wind pattern and topography indicate regions over which orographic lifting may occurs, corroborated by monthly mean UTH distribution. For example, high UTHs are observed over central Africa, western coast around Guinea, and Ethiopian highlands. From upper easterly winds and UTH pattern, it can be deduced that upper troposphere over tropical Atlantic Ocean may be influenced by cloud and moisture detrained from deep convection centers over West Africa.

Diurnal amplitudes and phases of precipitation index, cirrus anvil cloud, UTH, and MTH are represented in Fig. 5. Large diurnal

variations are observed over central Africa, western coast around Guinea, and Ethiopian highlands (Duvel and Kandel, 1985; Duvel, 1989; Machado et al., 1993). By contrast convectively inactive subtropical regions do not show meaningful diurnal variations. Despite smaller amplitude, discernible diurnal variations are observed over convergence zone of Atlantic Ocean.

Harmonic analysis indicates that rainfall over land tends to peak generally in the late afternoon and early evening, preceding cirrus anvil cloud maximum. Despite the height difference, UTH and MTH show nearly an identical peak. Free tropospheric humidity over land reaches its maximum in the nighttime similar to cirrus anvil cloud, lagging precipitation and high cloud (not shown). Over ocean, morning preference of rainfall is evident except for near the African coast. However, cirrus anvil cloud (and high cloud) attain maximum cloud fraction in the late afternoon. UTH and MTH over ocean tends to peak around midnight, a few hours after cirrus anvil cloud reaches maximum fraction.

Fig. 6 shows the spatial-mean diurnal anomalies of precipitation, cirrus anvil cloud, UTH, and MTH with vertical bars representing the standard error for each hourly mean. Average rainfall anomaly over land increases rapidly after noon and reaches maximum around 1800 LT. After attaining the peak, precipitation starts to decrease and reaches the minimum around noon. Maximum cirrus anvil cloud fraction is observed during nighttime (~0300 LT) with minimum near noon. Diurnal variation of high cloud is nearly in phase with that of cirrus anvil cloud except for broad peak in the evening (not shown), suggesting increase in lower and colder cloud at night (Soden, 2000; Machado et al., 2002). It was found that small convective cloud cells develop between noon and 1500 LT and grow or merge into larger clusters later over West Africa (Machado et al., 1993). UTH and MTH are higher during nighttime than daytime similar to cirrus anvil cloud. Minima of free tropospheric humidity are observed between 1500 LT and 1800 LT, just before the time of rainfall peak.

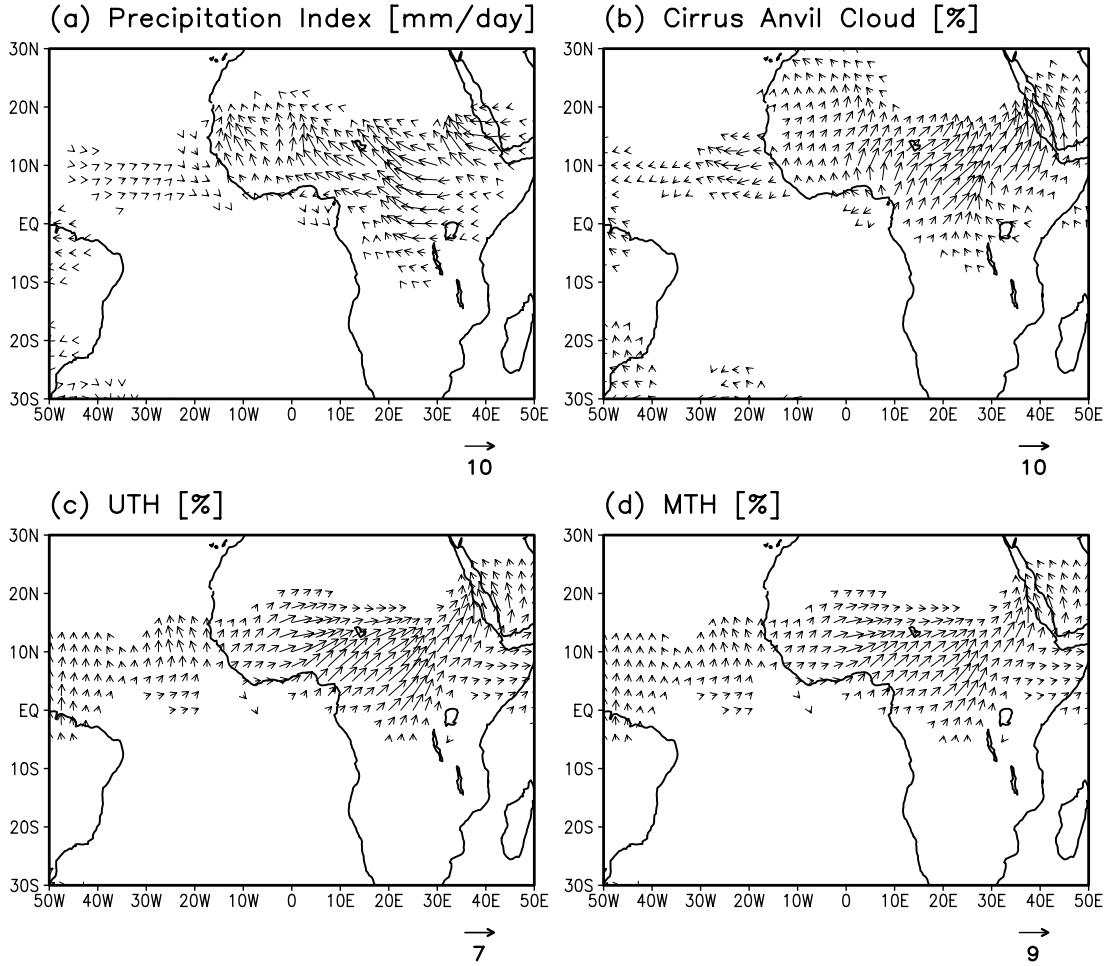

Figure 5: Diurnal amplitudes and phases of (a) precipitation, (b) cirrus anvil cloud, (c) UTH, and (d) MTH for July 2004. The length of the arrow depicts the diurnal amplitudes (10 mm day^{-1} for precipitation, 10% for cirrus anvil cloud, 7% for UTH, and 9% for MTH).

Convective regions of the Atlantic Ocean show an early morning peak of rainfall. In contrast, cirrus anvil cloud and high cloud attain a maximum cloud fraction in the late afternoon (~1800 LT). Unlike the land case, cirrus anvil cloud and high cloud decrease after reaching the peak. Machado et al. (1993) showed that while colder clouds over the Atlantic Ocean have a weak maximum coverage in early morning, warmer cloud fraction increase in the afternoon. This diurnal behavior was ascribed to large cold cloud clusters, thereby suggesting that internal variation of large convective systems is the main reason for the diurnal variation over ocean (Machado et al., 1993). Diurnal anomalies of UTH and MTH show a broad peak during nighttime starting from just after cirrus anvil cloud and high cloud reach the maximum. Minima of free tropospheric humidity are found between 1200 LT and 1500 LT, implying development of convective activity over ocean.

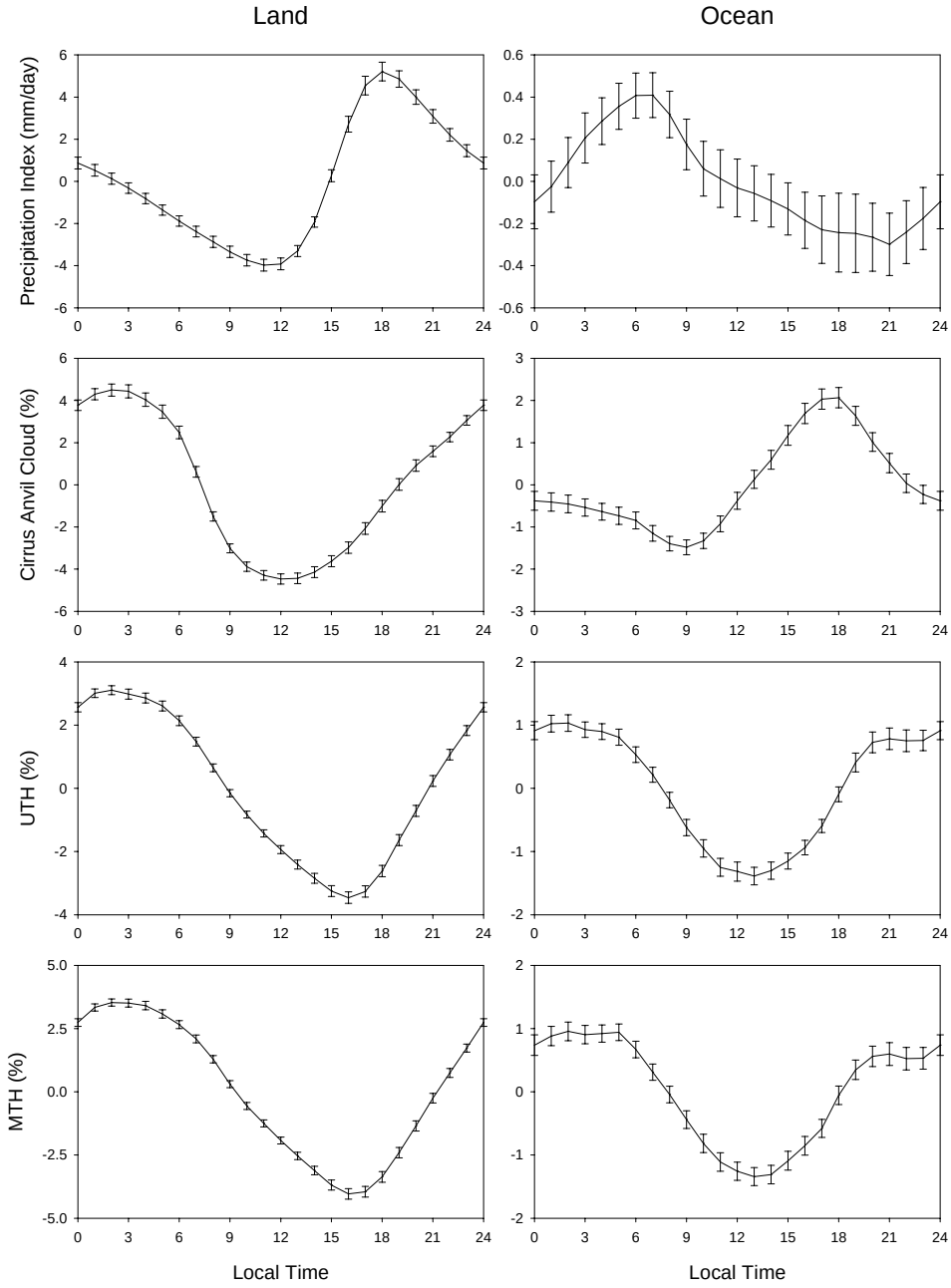

Figure 6: Average diurnal anomalies in precipitation (mm day^{-1}), cirrus anvil cloud (%), UTH (%), and MTH (%) for spatial averages over land regions (left) and ocean regions (right) in July 2004. Vertical bars represent the standard errors for each hourly mean.

4. DISCUSSION AND SUMMARY

Large diurnal amplitudes of precipitation and cirrus anvil cloud are observed over the convectively active regions such as Asian monsoon regions, central Africa, Ethiopian highlands, and western coast of Africa near Guinea. Over the land, precipitation maximums are generally observed in the late afternoon to early evening (~1800 LT) due to the afternoon boundary layer destabilization. During the day, solar heating over the land surface increases temperature of the adjacent lower-troposphere and thus enhances the atmospheric instability, resulting in convection development. In contrast, nocturnal radiative cooling of the land surface enhances the stability and thereby suppresses convection. Maximum cirrus anvil cloud fraction over land is observed during nighttime (~0300 LT) with a minimum near noon. High cloud shows a similar phase pattern except for a broad peak in the evening, suggesting that higher and colder clouds (e.g., deep convective clouds) evolve to lower and warmer clouds (cirrus anvil clouds or middle clouds) during the night (Soden, 2000; Machado et al., 2002).

Although diurnal amplitudes over the ocean are smaller than those over the land, discernible diurnal variations are found over coastal regions and convergence zones over the open ocean. It was shown that precipitation maximum around noon occurred over the west coast of Africa and the Bay of Bengal. The land may affect amplitudes as well as the timing of maximum in diurnal variation over the bay (Zuidema, 2003). By contrast, early morning precipitation maximum is observed over the open ocean, agreeing with the previous studies using passive microwave precipitation data (Imaoka and Spencer, 2000; Nesbitt and Zipser, 2003). Several possible mechanisms were suggested to explain oceanic deep convection (Gray and Jacobson, 1977; Randall et al., 1991; Chen and Houze, 1997). While the slight time lag between precipitation maximum and high cloud maximum is observed over land, ocean shows a nearly out-of-phase relationship between precipitation and high cloud. Over the ocean, high cloud and cirrus anvil cloud have nearly identical peak in the late afternoon (~1800 LT), implying that high cloud is composed of warmer (and lower) clouds.

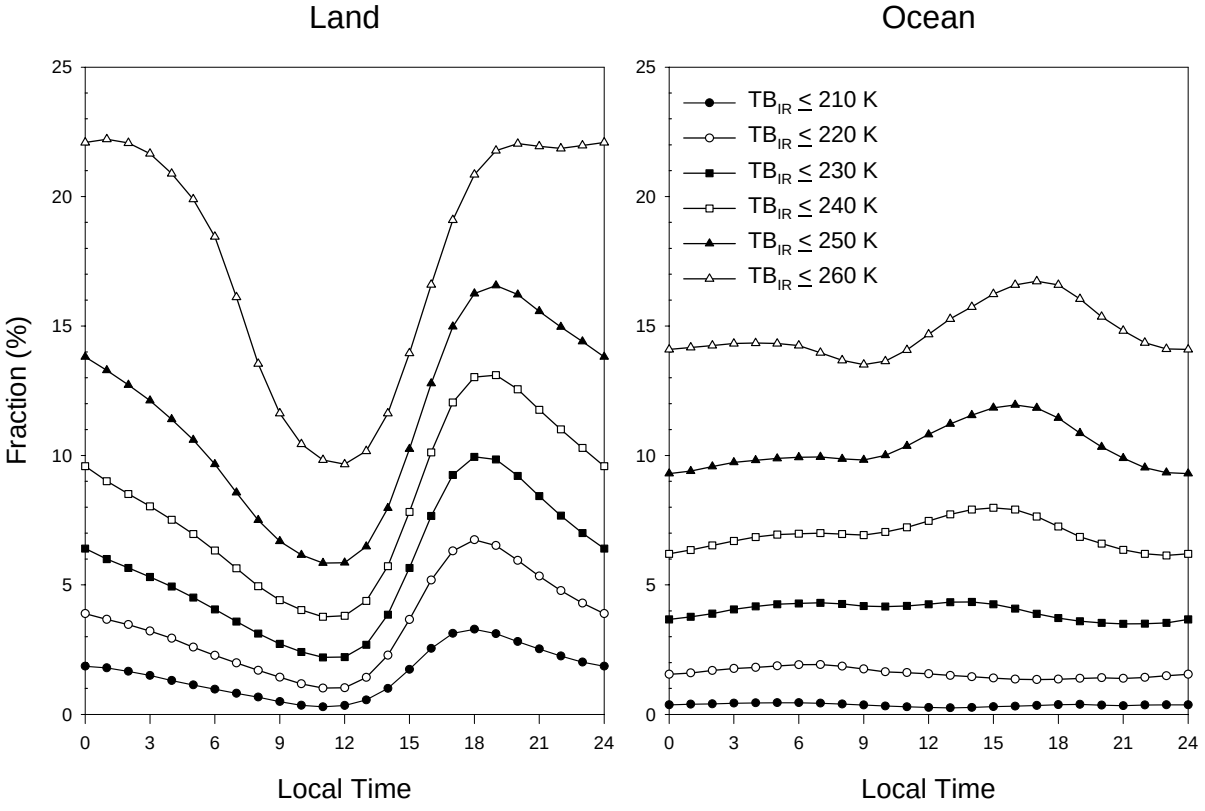

Figure 7: Hourly average cloud fraction for the brightness temperature threshold of 210 K, 220 K, 230 K, 240 K, 250 K, and 260 K over tropical Africa in July 2004. Left and right panels represent land and ocean, respectively.

Similar to precipitation and high cloud, water vapor in the upper troposphere (and middle troposphere) also shows noticeable diurnal variation over the convective regions with relatively larger diurnal amplitude over land. While a distinct peak centered at 0300 LT is found over land, ocean shows a broad peak during nighttime. This broad peak of UTH during the night might be partially explained by large-scale advection (Fig.4). Both land and ocean show time differences between UTH/MTH maximum and precipitation/high cloud. Over land (ocean), UTH and MTH lag precipitation by 9 hours (12-15 hours), and high cloud by 3 hours (3-6 hours). It was suggested that the diurnal variation of UTH is mainly influenced by the diurnal cycle of deep convection and high cloud from this phase lag relationship, implying moistening of the upper troposphere by the evaporation of hydrometeors detrained from deep convection centers (Soden, 2000; Tian et al., 2004).

However, a Lagrangian study doubted this traditional view of direct evaporation of cirrus cloud, because Lagrangian UTH tendencies and high cloud tendencies have the same phase (Soden, 2004). In addition, a cloud-masking effect was suggested for one of the possible reasons of time lag between high cloud and UTH (Udelhofen and Hartmann, 1995; Soden, 2004). Instead of direct moistening by evaporation of cloud condensates, the same dynamical mechanisms responsible for the formation and maintenance of high cloud was ascribed to the moistening and drying of upper troposphere (Soden, 2004). Compared to high cloud, cirrus anvil cloud show nearly identical peak to those of UTH and MTH (Fig. 3 and Fig. 6), supporting the notion that the same vertical-transport processes appear to influence both high cloud and free tropospheric humidity. However, hourly average cloud fraction for various temperature thresholds indicates that higher and colder clouds evolve to lower clouds during the nighttime especially over land (Fig. 7). Thus, it might be inferred that direct evaporation of cloud condensates moistens the free troposphere concurrently. It was shown that area expansions of convective cloud systems are affected not only by the upper-level divergence but also by the condensation-evaporation process (Machado and Laurent, 2004).

Meanwhile, UTH (and MTH) shows diurnal minimum just before the peak of precipitation over land. In contrast, UTH minimum lags the peak of precipitation and leads the time of high cloud maximum over ocean, implying the insignificant influence of diurnal variation of precipitation on UTH diurnal cycle. Instead, higher free tropospheric humidity during night appears to provide more favorable environment for cloud development (Machado et al., 1993; Nesbitt and Zipser, 2003).

5. ACKNOWLEDGEMENTS

This study has been supported by Korean Geostationary Program (COMS) through the fund granted by Korean Meteorological Administration (KMA).

6. REFERENCES

Bates, J. J., D. L. Jackson, F.-M. Breon, and Z. D. Bergen, 2001: Variability of tropical upper tropospheric humidity 1989-1998. *J. Geophys. Res.*, **106**, 32,271-32,281.

Chen, S. S., and R. A. Houze Jr., 1997: Diurnal variation and life-cycle of deep convective systems over the tropical Pacific warm pool. *Quart. J. Roy. Meteor. Soc.*, **123**, 357-388.

Dai, A., 2001: Global precipitation and thunderstorm frequencies. Part II: Diurnal variations. *J. Climate*, **14**, 1112-1128.

Dai, A., J. Wang, R. H. Ware, and T. Van Hove, 2002: Diurnal variation in water vapor over North America and its implications for sampling errors in radiosonde humidity. *J. Geophys. Res.*, **107**, 4090, doi:10.1029/2001JD000642.

Duvel, J. P., 1989: Convection over tropical Africa and the Atlantic Ocean during northern summer. Part I: Interannual and diurnal variations. *Mon. Wea. Rev.*, **117**, 2782-2799.

Duvel, J. P., and R. S. Kandel, 1985: Regional-scale diurnal variations of outgoing infrared radiation observed by METEOSAT. *J. Climate Appl. Meteor.*, **24**, 335-349.

Gambheer., A. V., and G. S. Bhat, 2001: Diurnal variation of deep cloud systems over the Indian region using INSAT-1B pixel data. *Meteor. Atmos. Phys.*, **78**, 215-225.

Gray, W. M., and R. W. Jacobson, 1977: The diurnal march of convective cloudiness over the Americas. *Mon. Wea. Rev.*, **105**, 1171-1188.

Hendon, H. H., and K. Woodberry, 1993: The diurnal cycle of tropical convection. *J. Geophys. Res.*, **98**, 16,623-16,637.

Imaoka, K., and R. W. Spencer, 2000: Diurnal variation of precipitation over the tropical oceans observed by TRMM/TMI combined with SSM/I. *J. Climate*, **12**, 4149-4158.

Kalnay, E., and Coauthors, 1996: The NCEP/NCAR 40-Year Reanalysis Project. *Bull. Amer. Meteor. Soc.*, **77**, 437-471.

Kondragunta, C. R., and A. Gruber, 1996: Seasonal and annual variability of the

diurnal cycle of clouds. *J. Geophys. Res.*, **101**, 21,377-21,390.

Machado, L. A. T., and H. Laurent, 2004: The convective system area expansion over Amazonia and its relationships with convective system life duration and high-level wind divergence. *Mon. Wea. Rev.*, **132**, 714-725.

Machado, L. A. T., J. P. Duvel, and M. Desbois, 1993: Diurnal variations and modulation by easterly waves of the size distribution of convective cloud clusters over west Africa and the Atlantic Ocean. *Mon. Wea. Rev.*, **121**, 37-49.

Machado, L. A. T., H. Laurent, and A. A. Lima, 2002: Diurnal march of the convection ovserved during TRMM-WETAMC/LBA. *J. Geophys. Res.*, **107**, D20, 8064, doi:10.1029/2001JD000338.

Nesbitt, S. W., and E. J. Zipser, 2003: The diurnal cycle of rainfall and convective intensity according to three years of TRMM measurements. *J. Climate*, **16**, 1456-1475.

Randall, D. A., Harshvardhan, and D. A. Dazlich, 1991: Diurnal variability of the hydrological cycle in a general circulation model. *J. Atmos. Sci.*, **48**, 40-62.

Schmetz, J., C. Geijo, W. P. Menzel, K. Strabala, L. van de Berg, K. Holmlund and S. Tjemkes, 1995: Satellite observations of upper tropospheric relative humidity, clouds and wind field divergence. *Contrib. Atmos. Phys.*, **68**, 345-357.

Schmetz, J., P. Pili, S. Tjemkes, D. Just, J. Kerkmann, S. Rota, and A. Ratier, 2002: An introduction to Meteosat Second Generation (MSG). *Bull. Amer. Meteor. Soc.*, **83**, 977-994.

Soden, B. J., 2000: Diurnal cycle of convection, clouds, and water vapor in the tropical upper troposphere. *Geophys. Res. Lett.*, **27**, 2173-2176.

Soden, B. J., 2004: The impact of tropical convection and cirrus on upper tropospheric humidity: A Lagrangian analysis of satellite measurements. *Geophys. Res. Lett.*, **31**, L20104, doi:10.1029/2004GL02980.

Soden, B. J., and F. P. Bretherton, 1993: Upper tropospheric relative humidity from the GOES 6.7 μm channel: Method and climatology for July 1987. *J. Geophys. Res.*, **98**, 16,669-16,688.

Sohn, B. J., and J. Schmetz, 2004: Water vapor-induced OLR variations associated with high cloud changes over the Tropics: A study from Meteosat-5 observations. *J. Climate*, **17**, 1987-1996.

Sohn, B. J., J. Schmetz, S. Tjemkes, M. König, H. J. Lutz, A. Arriaga, and E. S. Chung, 2000: Intercalibration of the Meteosat-7 water vapor channel with SSM/T-2. *J. Geophys. Res.*, **105**, 15,673-15,680.

Tian, B., B. J. Soden, and X. Wu, 2004: Diurnal cycle of convection, clouds, and water vapor in the tropical upper troposphere: Satellite versus a general circulation model. *J. Geophys. Res.*, **109**, D10101, doi:10.1029/2003JD004117.

Udelhofen, P. M., and D. L. Hartmann, 1995: Influence of tropical cloud systems on the relative humidity in the upper troposphere. *J. Geophys. Res.*, **100**, 7423-7440.

Yang, G.-Y., and J. M. Slingo, 2001: The diurnal cycle in the tropics. *Mon. Wea. Rev.*, **129**, 784-801.

Zuidema, P., 2003: Convective clouds over the Bay of Bengal. *Mon. Wea. Rev.*, **131**, 780-798.